Journal of Sound and Vibration (2002) **255**(4), 719–740
doi:10.1006/jsvi.2001.4186, available online at http://www.idealibrary.com on IDEAL®

CHAOS AND CHAOS SYNCHRONIZATION OF A SYMMETRIC GYRO WITH LINEAR-PLUS-CUBIC DAMPING

H.-K. CHEN

Department of Industrial Management, Hsiuping Institute of Technology, No. 11, *Gungye Road, Dali City, Taichung, Taiwan, Republic of China. E-mail: kanechen@giga.net.tw*

(*Received* 5 *September* 2001, *in final form* 4 *January* 2002)

The dynamic behavior of a symmetric gyro with linear-plus-cubic damping, which is subjected to a harmonic excitation, is studied in this paper. The Liapunov direct method has been used to obtain the sufficient conditions of the stability of the equilibrium points of the system. By applying numerical results, time history, phase diagrams, Poincaré maps, Liapunov exponents and Liapunov dimensions are presented to observe periodic and chaotic motions. Besides, several control methods, the delayed feedback control, the addition of constant motor torque, the addition of period force, and adaptive control algorithm (ACA), have been used to control chaos effectively. Finally, attention is shifted to the synchronization of chaos in the two identical chaotic motions of symmetric gyros. The results show that one can make two identical chaotic systems to synchronize through applying four different kinds of one-way coupling. Furthermore, the synchronization time is also examined.

1. INTRODUCTION

Research in the area of gyro dynamics dates back about one hundred years. Gyroscope is an attractive and everlasting subject of dynamics, which has been studied by many authors. Beyond its purely scientific interest, the gyroscope has attributes of great utility to navigational, aeronautical and space engineering. The pioneering paper on the concept of chaotic motion in gyros was not presented until 1981 [1]. Recently, Ge *et al.* [2, 3] conducted a detailed study evaluating the non-linear behavior of a symmetric heavy gyroscope mounted on a vibrating base. In their study, the chaotic motion of the system with linear damping was investigated. Very recently, the motion of a symmetric gyro, which is subjected to a harmonic vertical base excitation has been studied by Tong and Mrad [4], with particular emphasis on its non-linear dynamic behavior. However, their study did not take the damping effect into account. Their results also indicate that a symmetric gyro exhibits both regular and chaotic motions. The type of the attractors (fixed point, periodic, quasi-periodic, chaotic) is also encountered. Therefore, analyzing the dynamics of gyro using the chaotic method is a relatively new approach. In this paper, the dynamic behaviors of a symmetric gyro with linear-plus-cubic damping which is subjected to a harmonic excitation will be studied in detail.

The concept of chaos was first introduced by Poincaré [5] to describe orbits in space mechanics. The chaotic behaviors of fluid were given by Lorenz [6]. Chaos occurs in mechanical or electrical oscillators, in rotating heated fluids, in chemical reactions, even in economic systems, etc.

0022-460X/02/$35.00

In this work, the stability of the equilibrium points of the system is investigated by the Liapunov direct method. Bifurcation of the parameter-dependent system is studied numerically. The time evolutions of the non-linear dynamical system responses are described in phase portraits via the Poincaré map technique. The occurrence and the nature of chaotic attractors are verified by evaluating Liapunov exponents and Liapunov dimensions.

The presence of chaotic behavior is generic for suitable non-linearity, ranges of parameters and external forces, where one wishes to avoid or control so as to improve the performance of a dynamical system. Sometimes chaos is useful, as in mixing process or in heat transfer. However, chaos is always unwanted or undesirable. Clearly, the ability to control chaos, that is to convert chaotic oscillations into desired regular ones with a periodic time dependence, would be beneficial in working with a particular system. It is thus of great practical importance to develop suitable control methods. Recently, much interest has been focused on this type of problem—controlling chaos [7–9]. The aim of this paper is to control chaotic motion of the gyroscope. For this purpose, many control methods, which are the delayed feedback control, the addition of the constant motor torque, the addition of the periodic force, and adaptive control algorithm (ACA), are used to control chaos.

The problem of synchronization of dynamical system is one of the classical topics in engineering science. Recently, renewed interest in this field was stimulated in connection with the synchronization of chaotic motion. If two identical copies of a chaotic system are started with similar initial conditions, their motions will not remain similar for long. Since exponential divergence of orbits will amplify for any initial small errors. It appears, at first, that it would be very difficult to keep both copies of a chaotic system synchronized. But, in 1990, Pecora and Carroll [10] showed that synchronization was indeed possible, and moreover, it could be achieved with a simple coupling. Because of their works, the synchronization of chaotic dynamical systems has been intensively studied by other researchers [11]. The basic idea in identical synchronization is to take two copies of fixed chaotic system and let one control the other. The master (drive) system provides a signal that is fed to the slave (response) system. The signal is usually one of the co-ordinates of the master chaotic system. Synchronization can be thought of as a form of control chaos. Finally, attention is shifted to the synchronization of chaos in the symmetric gyros. For this purpose, four different kinds of one-way coupling are adopted to perform the synchronizing chaotic motion. The synchronization of chaos will be also shown by phase trajectory. The sign of the sub-Liapunov exponent is also applied to diagnose whether synchronization of chaos occurs or not. Four different kinds of one-way coupling are used to examine whether the two identical chaotic systems will be synchronized or not. Moreover, the synchronization time is also examined.

2. EQUATIONS OF MOTION

The geometry of the problem under consideration is depicted in Figure 1. The motion of a symmetric gyro mounted on a vibrating base can be described by Euler's angles θ (nutation), ϕ (precession), and ψ (spin). By using Lagrangian approach, the Lagrangian has the expression

$$L = \tfrac{1}{2} I_1 (\theta^2 + \dot{\phi}^2 \sin^2\theta) + \tfrac{1}{2} I_3 (\dot{\phi}\cos\theta + \dot{\psi})^2 - M_g(\ell + \bar{\ell}\sin\omega t)\cos\theta, \tag{1}$$

where I_1 and I_3 are the polar and equatorial moments of inertia of the symmetric gyro, respectively, M_g is the gravity force, $\bar{\ell}$ is the amplitude of the external excitation disturbance,

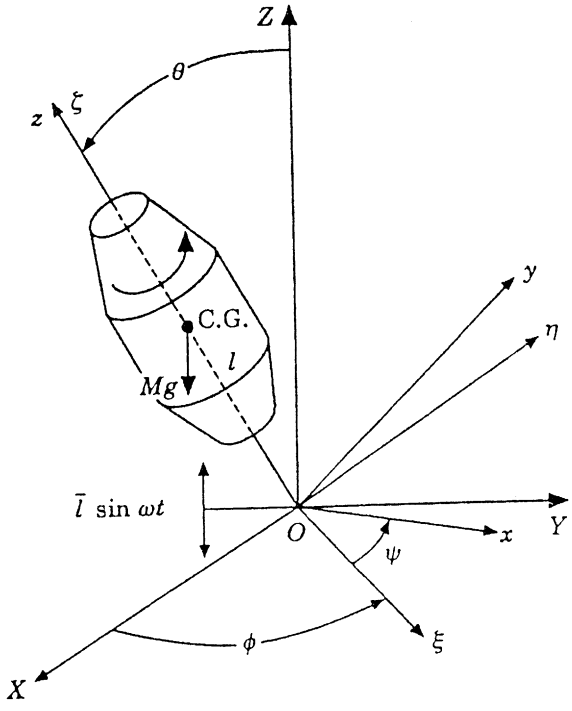

Figure 1. A schematic diagram of the physical system.

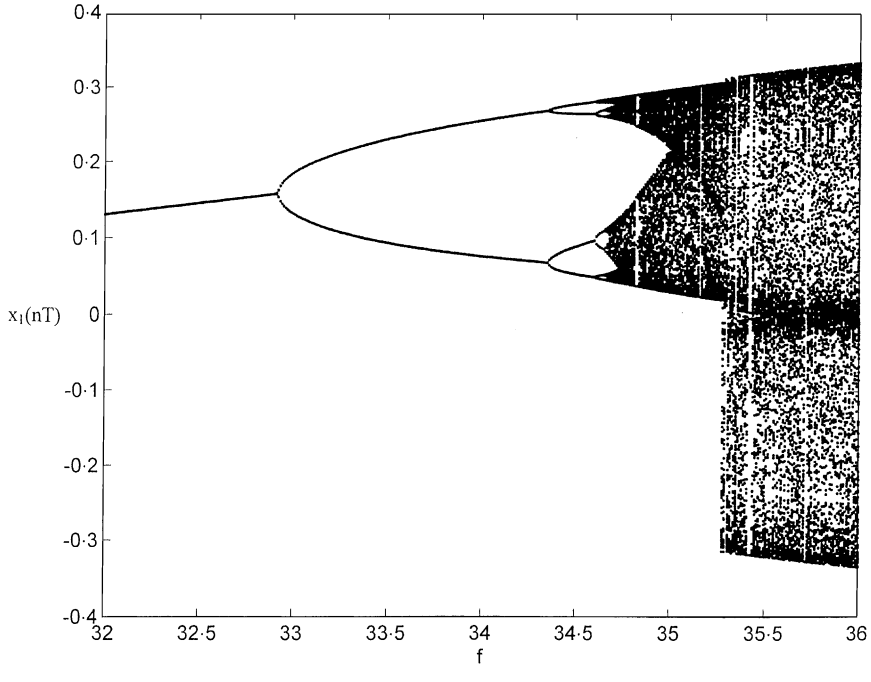

Figure 2. Bifurcation diagrams for specific values set ($\alpha^2 = 100$, $\beta = 1$ $c_1 = 0{\cdot}5$, $c_2 = 0{\cdot}05$, $\omega = 2$); steady state angular position $x_1(nT)$ versus the normalized amplitude f of harmonic excitation.

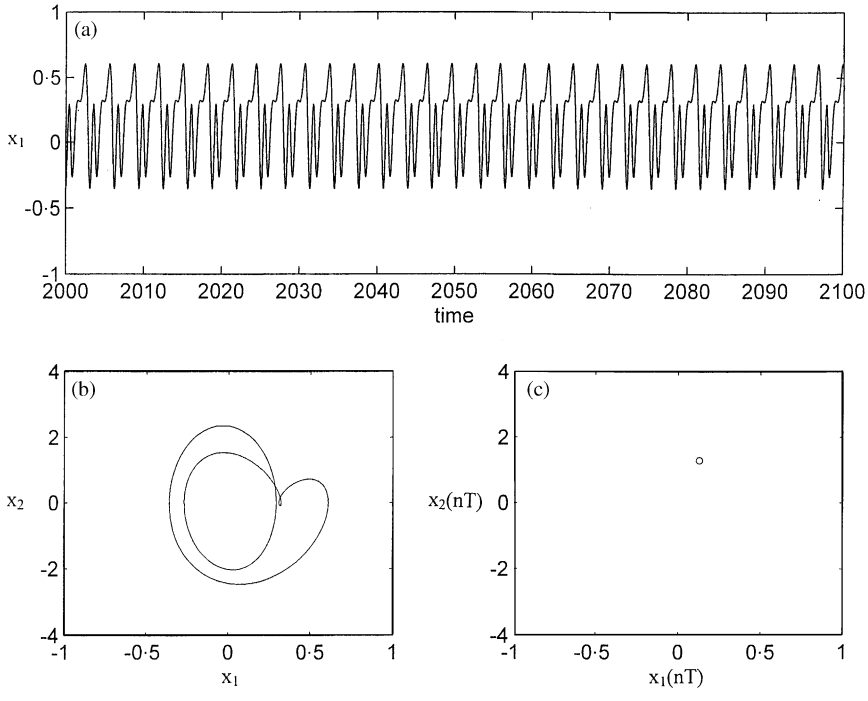

Figure 3. (a) Time history, (b) Phase trajectory, (c) Poincaré map for $f = 32{\cdot}0$ (period-1T).

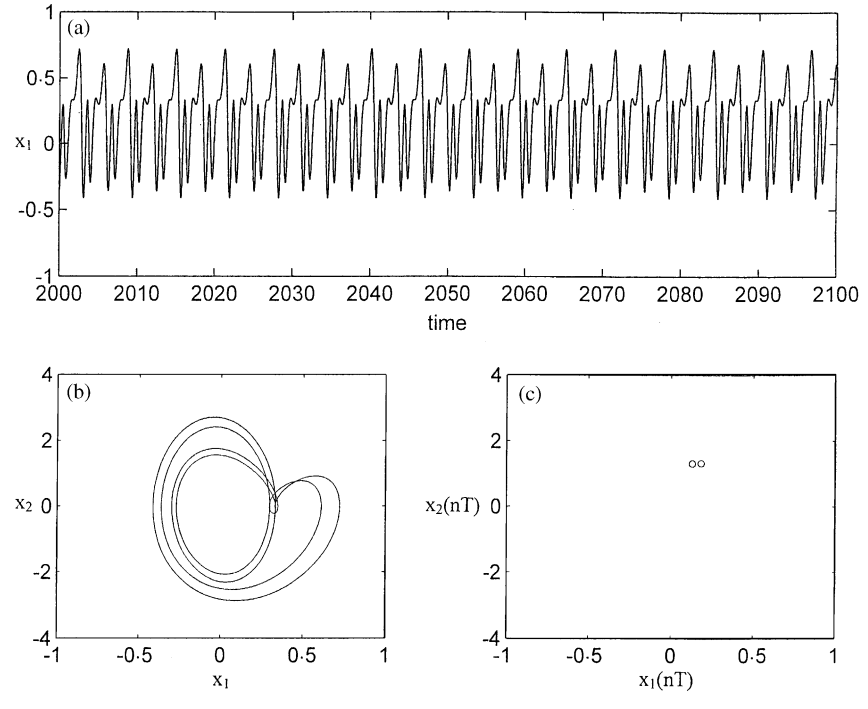

Figure 4. (a) Time history, (b) Phase trajectory, (c) Poincaré map for $f = 33{\cdot}0$ (period-2T).

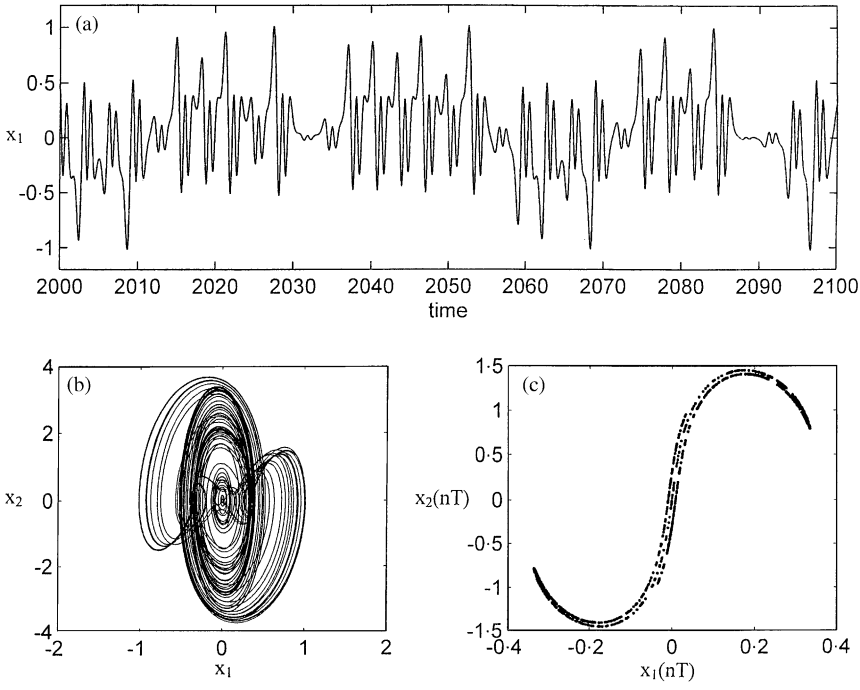

Figure 5. (a) Time history, (b) Phase trajectory, (c) Poincaré map for $f = 36{\cdot}0$ (chaos).

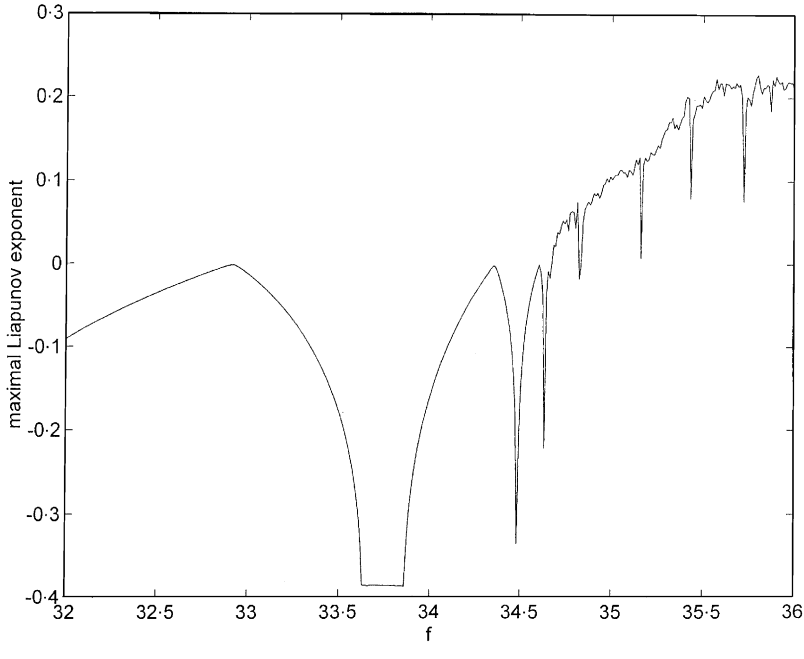

Figure 6. The maximal Liapunov exponents as a function of f.

and ω is the frequency of the external excitation disturbance. It is not difficult to see that co-ordinates ϕ and ψ are cyclic, as they are absent from the Lagrangian, which provides us with two first integrals of the motion expressing the conjugate momenta. The momentum integrals are

$$P_\phi = \frac{\partial L}{\partial \dot{\phi}} = I_1 \dot{\phi} \sin^2\theta + I_3(\dot{\phi}\cos\theta + \dot{\psi})\cos\theta = \beta_\phi, \tag{2}$$

$$P_\psi = \frac{\partial L}{\partial \dot{\psi}} = I_3(\dot{\phi}\cos\theta + \dot{\psi}) = I_3\omega_z = \beta_\psi, \tag{3}$$

where ω_z is the spin velocity of the gyro.

The Routh's procedure is adopted along with the above-mentioned relations, the Routhian of the system becomes

$$R = L - \beta_\phi\dot{\phi} - \beta_\psi\dot{\psi} = \tfrac{1}{2} I_1\dot{\theta}^2 - \left[\frac{(\beta_\phi - \beta_\psi\cos\theta)^2}{2I_1\sin^2\theta} + \frac{\beta_\phi^2}{2I_3} + M_g(\ell + \bar{\ell}\sin\omega t)\cos\theta\right]. \tag{4}$$

The equation above depends on the angle θ alone. According to Gantmacher [12], $\beta_\phi = \beta_\psi$ when $\theta = 0$. The dissipative force is also assumed to be in linear-plus-cubic form, which is

$$F = -D_1\dot{\theta} - D_2\dot{\theta}^3, \tag{5}$$

where D_1 and D_2 are positive constants.

The only equation of motion describing the system can be obtained from

$$\frac{\mathrm{d}}{\mathrm{d}t}\left(\frac{\partial R}{\partial \dot{\theta}}\right) - \frac{\partial R}{\partial \theta} = F. \tag{6}$$

The equation above allows the system to be viewed as a single-degree-of-freedom system. The equation governing the gyroscope is given by

$$\ddot{\theta} + \frac{\beta_\phi^2}{I_1^2}\frac{(1-\cos\theta)^2}{\sin^3\theta} + \frac{D_1}{I_1}\dot{\theta} + \frac{D_2}{I_1}\dot{\theta}^3 - \frac{M_g\ell}{I_1}\sin\theta = \frac{M_g\bar{\ell}}{I_1}\sin\omega t\sin\theta. \tag{7}$$

The normalized equations in convenient first order form are

$$\begin{aligned} \dot{x}_1 &= x_2, \\ \dot{x}_2 &= -\alpha^2\frac{(1-\cos x_1)^2}{\sin^3 x_1} - c_1x_2 - c_2x_2^3 + \beta\sin x_1 + f\sin\omega t\sin x_1, \end{aligned} \tag{8}$$

where

$$x_1 = \theta, \quad x_2 = \dot{\theta}, \quad \alpha = \frac{\beta_\phi}{I_1} = \frac{I_3\omega_z}{I_1}, \quad c_1 = \frac{D_1}{I_1}, \quad c_2 = \frac{D_2}{I_1}, \quad \beta = \frac{M_g\ell}{I_1}, \quad f = \frac{M_g\bar{\ell}}{I_1}. \tag{9}$$

3. STABILITY ANALYSIS BY LIAPUNOV DIRECT METHOD

In this section, the stability of the equilibrium points of the system is investigated by the Liapunov direct method. The equations of motion given in previous section are

deterministic, second order, non-linear and non-autonomous. It is a highly non-linear problem. For this purpose, the non-linear terms $(1-\cos x_1)^2/\sin^3 x_1$ and $\sin x_1$ are expanded into power series of x_1:

$$\frac{(1-\cos x_1)^2}{\sin^3 x_1} = \frac{x_1}{4} + \frac{x_1^3}{12} + O(x_1)^5, \tag{10}$$

$$\sin x_1 = x_1 - \frac{x_1^3}{6} + O(x_1)^5. \tag{11}$$

Using equations (10) and (11), the governing equations of the system can be expressed as

$$\begin{aligned} \dot{x}_1 &= x_2, \\ \dot{x}_2 &= -P(t)x_1 - c_1 x_2 - c_2 x_2^3 + Q(t)x_1^3 + O(x_1)^5, \end{aligned} \tag{12}$$

where

$$P(t) = \frac{\alpha^2}{4} - \beta - f\sin\omega t, \quad Q(t) = \frac{\alpha^2}{12} - \frac{\beta}{6} - \frac{f\sin\omega t}{6}. \tag{13}$$

Using the Liapunov stability analysis [13], the fixed points of the system are first examined. It can be seen that (A) $x_1 = x_2 = 0$ and (B) $x_1 = \pi$, $x_2 = 0$ are fixed points for all parameter values.

For the fixed point (A) $(x_1, x_2) = (0, 0)$, this solution describes a motion in which one of the principal axes of the gyro coincides with the local vertical axis. To study the stability of the equilibrium point of the system, the disturbance of motion is set to be

$$x_1 = \xi_1, \quad x_2 = \xi_2. \tag{14}$$

Substituting equation (14) into equation (12), the equations of disturbance become

$$\begin{aligned} \dot{\xi}_1 &= \xi_2, \\ \dot{\xi}_2 &= -P(t)\xi_1 - c_1\xi_2 - c_1\xi_2^3 + Q(t)\xi_1^3 + O(\xi_1)^5. \end{aligned} \tag{15}$$

In this case there is no physical intuition readily available to guide us in the choice of V. The Liapunov function is assumed to be

$$V(t, \xi_1, \xi_2) = \tfrac{1}{2}P(t)\,\xi_1^2 + \tfrac{1}{2}\xi_2^2 + \xi_1\xi_2. \tag{16}$$

The Liapunov function V is positive definite if it satisfies the inequality

$$\frac{\alpha^2}{4} - \beta - 1 > f. \tag{17}$$

The total derivative of $-\dot{V}(x)$ is

$$-\dot{V}(t, \xi_1, \xi_2) = \left[P(t) - \frac{f\omega}{2}\cos\omega t\right]\xi_1^2 + c_1\xi_1\xi_2 + (c_1 - 1)\,\xi_2^2 + O(\xi_i)^3. \tag{18}$$

The requirements for $\dot{V}$ in the Liapunov direct method are

$$c_1 > 1, \quad \frac{\alpha^2}{4} - \beta - \frac{c_1^2}{4(c_1-1)} > f\sqrt{1 + \frac{\omega^2}{4}}. \tag{19}$$

According to the Liapunov stability theorem and new theorem proposed by Cveticanin [14], inequalities (19) are sufficient conditions for system stability, and $(x_1, x_2) = (0, 0)$ is asymptotically stable equilibrium.

Similarly, the Liapunov function V for point (B) is taken as

$$V(t, \xi_1, \xi_2) = \tfrac{1}{2}(P - 3\pi^2 Q)\xi_1^2 + \tfrac{1}{2}\xi_2^2 + \xi_1\xi_2. \tag{20}$$

The following inequalities:

$$c_1 > 1, \quad \frac{\alpha^2}{4}(1 - \pi^2) + \left(\frac{\pi^2}{2} - 1\right)\beta > \left\{\frac{c_1^2}{4(c_1 - 1)} + f\sqrt{\left(\frac{\pi^2}{2} - 1\right)^2\left(1 + \frac{\omega^2}{4}\right)}\right\}, \tag{21}$$

are the sufficient conditions for system stability. The fixed point $(x_1, x_2) = (\pi, 0)$ is asymptotically stable equilibrium.

It is evident that stability has been established. In general, β and c_1 are fixed for a given system. However, the normalized amplitude f and the frequency of the external harmonic excitation ω and the spin velocity ω_z could be varied. An inspection of inequalities (19) indicates that stability can be achieved simply by increasing the spin velocity when the gyroscope is spinning in an upright position. This finding has practical importance for the design of gyroscope instruments. For instance, it is desirable to set the gyro in more stable spinning state by simply giving higher initial spinning velocity.

4. BIFURCATION DIAGRAM, PHASE PORTRAITS AND POINCARÉ MAP

In the present study, the non-linear equation of motion (8) is integrated numerically in order to obtain the various dynamic behaviors of the gyro. The bifurcation diagram provides a summary of essential dynamics and is therefore a useful method for acquiring this overview.

For this system, bifurcation can easily be detected by examining a graph of x_1 versus f. The bifurcation will be obtained by the fourth order Runge–Kutta numerical integration algorithm with a given set of initial conditions. The bifurcation diagram for specific value set $(\alpha^2 = 100, \quad \beta = 1, \quad c_1 = 0{\cdot}5, \quad c_2 = 0{\cdot}05, \quad \omega = 2)$ is presented in Figure 2. The period-doubling bifurcation phenomena can easily be observed. If f increases, the diagram becomes very complex. The Poincaré map is also used to examine the behavior of the system. It is a three-dimensional problem with x_1, x_2, and t as independent variables. The t is a multiple of T which is the period of the harmonic excitation and is defined as $T = 2\pi/\omega$.

Figures 3(a)–3(c) show the time history, the phase trajectory and the Poincaré map for $f = 32{\cdot}0$. As seen in Figure 3(c), there is only one data point and is denoted by symbol "o". Clearly, it indicates that the system is period-1T motion. Figures 4(a)–4(c) show the time history, the phase trajectory and the Poincaré map for $f = 33{\cdot}0$. Similarly, Figure 4(c) shows the system in a period 2 motion using two data points denoted by symbol "o". Figures 5(a)–5(c) show the time history, the phase trajectory and the Poincaré map for $f = 36{\cdot}0$. An interesting attractor, which configuration looks like "S", is presented. However, when the bifurcation diagram loses continuity, it means that the system is either in quasi-periodic motion or chaotic motion. Therefore, further tests are required to classify the dynamics.

5. LIAPUNOV EXPONENTS AND LIAPUNOV DIMENSIONS

According to the previous section, quantifying chaos has become an important problem. Liapunov exponents can provide qualitative and quantitative tests for dynamic

behavior. The algorithm developed by Wolf *et al.* [15] is used to determine the Liapunov exponents.

The Liapunov exponents may be used to measure the sensitive dependence of the initial conditions. Different solutions of a dynamic system, such as fixed point, periodic motion, quasi-periodic motion, and chaotic motion can be distinguished from it. If two trajectories start close to one another in phase space, they will move exponentially away from each other for small times on the average. Thus, if d_0 is a measure of the initial distance between the two starting points, the distance is $d(t) = d_0 2^{\lambda t}$. The symbol λ is called Liapunov exponent. The divergence of chaotic orbits can only be locally exponential, because if the system is bounded, $d(t)$ cannot grow to infinity. A measure of this divergence of orbits is that the exponential grown at many points along a trajectory has to be averaged. When $d(t)$ is too large, a new 'nearby' trajectory $d_0(t)$ is defined. The Liapunov exponent can be expressed as

$$\lambda = \frac{1}{t_N - t_0} \sum_{k=1}^{N} \log_2 \frac{d(t_k)}{d_0(t_{k-1})}. \tag{22}$$

The signs of the Liapunov exponents provide a qualitative picture of a system dynamics. The criterions are

$$\lambda > 0 \text{ (chaotic)},$$

$$\lambda \leqslant 0 \text{ (regular motion)}.$$

The periodic and chaotic motions can be distinguished from the bifurcation diagram, while the quasi-periodic motion and chaotic motion may be confused. However, they can be distinguished from the Liapunov exponent method.

For the system, if $x_3 = \omega t$ is introduced, then the non-autonomous equations (8) of motion can be transformed as autonomous one:

$$\begin{aligned} \dot{x}_1 &= x_2, \\ \dot{x}_2 &= -\alpha^2 \frac{(1 - \cos x_1)^2}{\sin^3 x_1} - c_1 x_2 - c_2 x_2^3 + \beta \sin x_1 + f \sin x_3 \sin x_1, \\ \dot{x}_3 &= \omega. \end{aligned} \tag{23}$$

For example, in the phase space (x_1, x_2, x_3), the Liapunov exponents for the system are found to be $(\lambda_1, \lambda_2, \lambda_3 = 0)$. The Liapunov spectra for specific system parameter value set $(\alpha^2 = 100,\ \beta = 1,\ c_1 = 0{\cdot}5,\ c_2 = 0{\cdot}05,\ \omega = 2)$ as $f = 32{\cdot}0$–$36{\cdot}0$ are shown in Figure 6 to confirm the chaotic dynamics.

There are a number of different fractional-dimension-like indices, e.g., the information dimension, Liapunov dimension, and correlation exponent, etc. The difference between them is often small. The Liapunov dimension is a measure of the complexity of the attractor. It was developed by Frederickson *et al.* [16]. The Liapunov dimension d_L is introduced as

$$d_L = j + \frac{\sum_{i=1}^{j} \lambda_i}{|\lambda_{j+1}|}, \tag{24}$$

where j is defined by the following conditions:

$$\sum_{i=1}^{j} \lambda_i > 0 \quad \text{and} \quad \sum_{i=1}^{j+1} \lambda_i < 0.$$

TABLE 1

Liapunov exponents and Liapunov dimensions of the system for different f

f	λ_1	λ_2	λ_3	$\sum\lambda_i$	d_L	
32.0	− 0·0906756	− 0·6384222	0	− 0·7290978	1	Period-1
33·0	− 0·0129279	− 0·7598052	0	− 0·7727331	1	Period-2
34·5	− 0·1495718	− 0·6363110	0	− 0·7858827	1	Period-4
36·0	0·2098415	− 1·0279003	0	− 0·8180588	1.29	Chaos

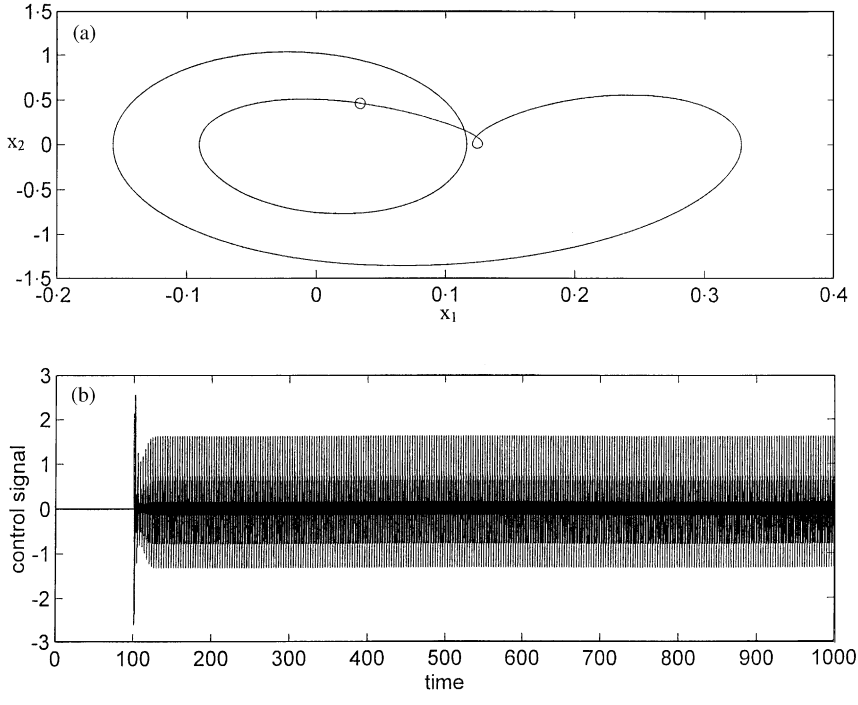

Figure 7. $K = 1{\cdot}0$ and $\tau = 2$, the period-1T motion of the system after feedback control.

The Liapunov dimension for a strange attractor is not a integer. The Liapunov dimensions and the Liapunov exponents of the non-linear system are listed in Table 1 for different values of f. It is also found that the summation of the Liapunov exponents of the system is not equal to $c_1 + c_2$. Because the system possesses the linear-plus-cubic damping.

6. CONTROLLING OF CHAOS

Several interesting non-linear dynamic behaviors of the system have been discussed in previous sections. It has been shown that the forced system exhibits both regular and chaotic motions. The extreme sensitivity to initial states in a system operating in chaotic mode can be very destructive to the system because of unpredictable behavior.

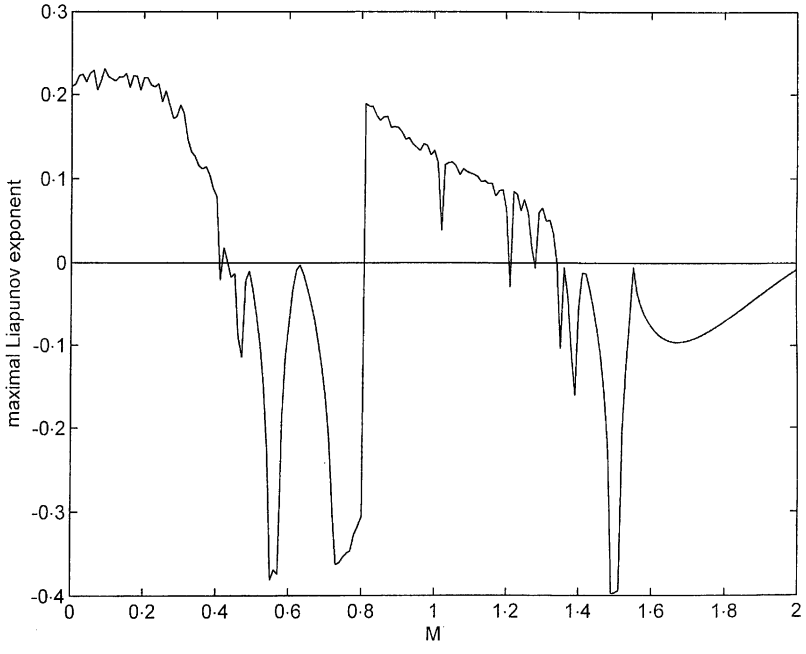

Figure 8. The maximal Liapunov exponents against M.

In order to improve the performance of a dynamic system or avoid the chaotic phenomena, we need to convert a chaotic motion to become a periodic motion. In this section, the focus is shifted to the control of the chaotic motion. For this purpose, the delayed feedback control, the addition of the constant motor torque, the addition periodic force, and adaptive control algorithm (ACA) are used to control chaos.

6.1. CONTROLLING OF CHAOS BY THE DELAYED FEEDBACK CONTROL

Let us consider a dynamic system, which can be simulated by ordinary differential equations. We imagine that the equations are unknown, but some scalar variable can be measured as a system output. The idea of this method is that the difference $D(t)$ between the delayed output signal $y(t-\tau)$ and the output signal $y(t)$ is used as a control signal. In other words, a perturbation form is adopted as

$$u(t) = K[y(t-\tau) - y(t)] = KD(t). \tag{25}$$

Here τ is delay time. By choosing an appropriate weight K and τ of the feedback control system one can achieve the periodic state. For $K = 1{\cdot}0$ and $\tau = 2$, after 100 s, the control scheme is activated and the system reaches to period-1 motion. The results are shown in Figure 7.

6.2. CONTROLLING OF CHAOS BY THE ADDITION OF THE CONSTANT MOTOR TORQUE

Interestingly, one can even add just a constant term to control or quench the chaotic attractor to a desired periodic one in the typical non-linear non-autonomous system. It

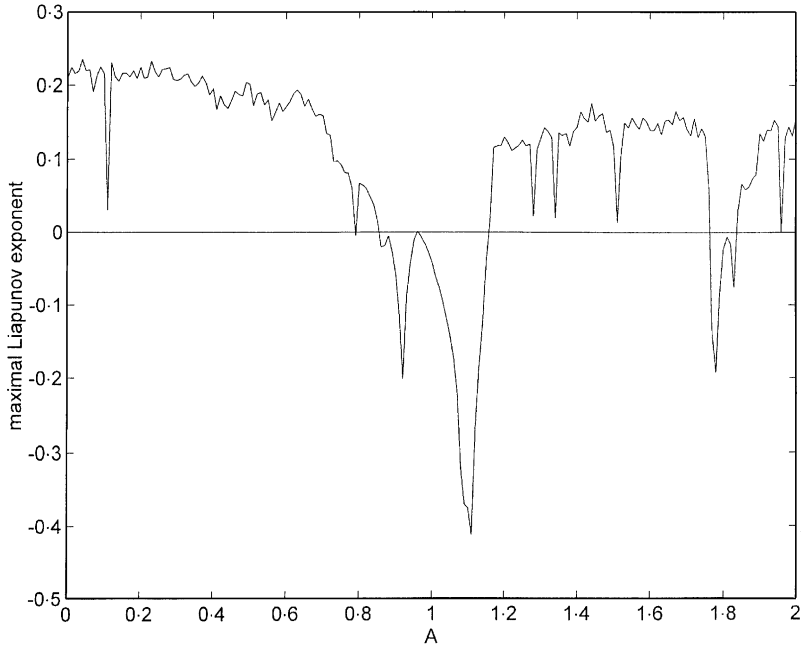

Figure 9. The maximal Liapunov exponents against A for fixed $\varpi = 1$.

ensures effective control in a very simple way. In order to understand this simple controlling approach in a better way, this method is applied numerically (8). The constant motor torque M is added into the second equation of equation (8).

If one considers the effect of the constant motor torque M by increasing it from zero upward, the chaotic behavior is altered. Spectral analysis of the Liapunov exponents has proven to be the most useful dynamical diagnostic tool for examining chaotic motions. In Figure 8, the maximal Liapunov exponents are shown. When the constant motor torque M is presented at certain interval, the system returns to regular motion.

6.3. CONTROLLING OF CHAOS BY THE ADDITION OF THE PERIODIC FORCE

The control of the system dynamic can be achieved by the addition of external periodic force in the chaotic state. The added periodic force $A \sin \varpi t$ is added into the second equation of equation (8). The system can be investigated by numerical solution, with the remaining parameters fixed. We examine the change of dynamics of the system as a function of A for fixed $\varpi = 1{\cdot}0$. The maximal Liapunov exponents are estimated numerically. The results are shown in Figure 9. At certain intervals, the maximal Liapunov exponents $\lambda_i \leqslant 0$, indicates that the motion of the system can now be predicted.

6.4. CONTROLLING OF CHAOS BY THE ADAPTIVE CONTROL ALGORITHM (ACA)

In 1990, Huberman and Lumer have suggested a simple and effective adaptive control algorithm, which utilizes an error signal proportional to the difference between the goal

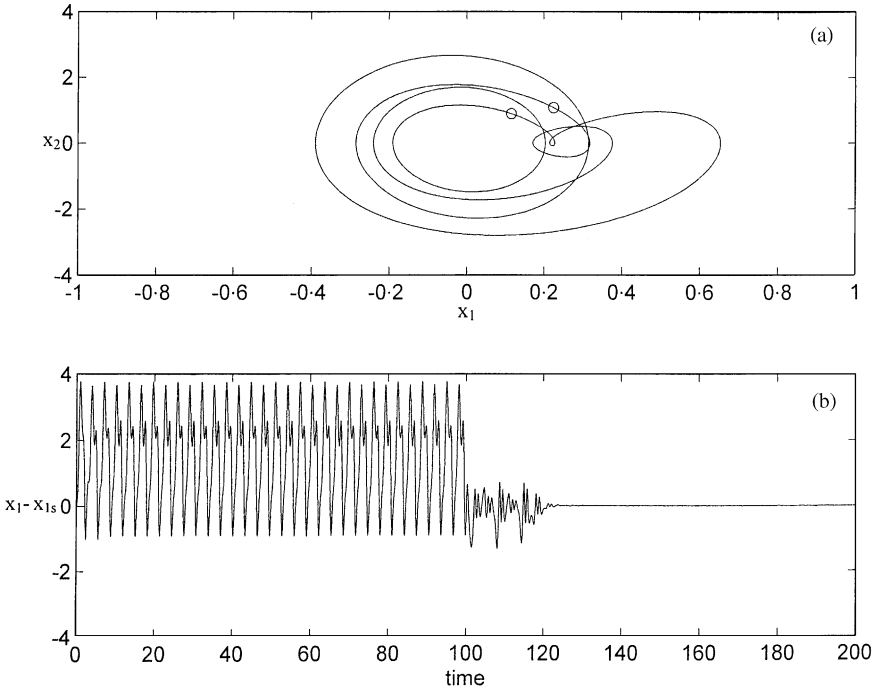

Figure 10. The period-2T motion applying adaptive control.

output and actual output of the system. The error signal governs the change of parameter of the system, which readjusts so as to reduce the error to zero. This method can be explained briefly: the system motion is set back to desired state X_s by adding dynamics on the control parameter P through the evolution equation below

$$\dot{P} = \varepsilon G(X - X_s), \tag{26}$$

where the function G depends on the difference between X_s and the actual output X, and ε indicates the stiffness of the control. The function G could be either linear or non-linear. In order to convert the dynamics of system (8), the α^2 term in equation (8) is replaced by

$$\dot{A} = \varepsilon[(x_1 - x_{1s}) + (x_2 - x_{2s})]. \tag{27}$$

If $\varepsilon = 0{\cdot}04$, the system can reach period-2T motion as indicated in Figure 10. It is clear that the desired periodic motion can be reached by adaptive control algorithm.

7. CHAOS SYNCHRONIZATION

Chaos synchronization is an important problem in the non-linear science. The chaos synchronization problem has the following feature: The trajectories of a slave (response) system must tracks the trajectories of a master (drive) system in spite of both master and slave system being different. In this section, we describe the linking of two chaotic systems with a one-way coupling. The state equations of two identical gyros with a one-way

coupling element are represented as

Drive (*master*):

$$\begin{aligned} \dot{x}_1 &= x_2, \\ \dot{x}_2 &= -\alpha^2 \frac{(1-\cos x_1)^2}{\sin^3 x_1} - c_1 x_2 - c_2 x_2^3 + \beta \sin x_1 + f \sin \omega t \sin x_1. \end{aligned} \tag{28}$$

Response (*slave*):

$$\begin{aligned} \dot{y}_1 &= y_2, \\ \dot{y}_2 &= -\alpha^2 \frac{(1-\cos y_1)^2}{\sin^3 y_1} - c_1 y_2 - c_2 y_2^3 + \beta \sin y_1 + f \sin \omega t \sin y_1 + \varepsilon F(x_2, y_2), \end{aligned} \tag{29}$$

where ε is the coupling parameter, $F(x_2, y_2)$ is the coupling function. In order to confirm synchronization of chaos, four different kinds of one-way coupling are introduced as follows:

(A) $\varepsilon F(x_2, y_2) = \varepsilon(x_2 - y_2)$,
(B) $\varepsilon F(x_2, y_2) = \varepsilon \sin(x_2 - y_2)$,
(C) $\varepsilon F(x_2, y_2) = \varepsilon[\exp(x_2 - y_2) - 1]$,
(D) $\varepsilon F(x_2, y_2) = \varepsilon \sinh(x_2 - y_2)$.

In fact, synchronization of chaos can be regarded as a special tracking problem, with the desired trajectory not being a constant (chaotic trajectory). Where the one-way coupling is a control scheme. When the synchronization occurs ($x_i(t) = y_i(t)$, $i = 1, 2$), otherwise they are different.

In order to study synchronization of chaos, the influence of the coupling strength on the two identical systems behavior will be examined by observing how the coupling parameter ε changes with the constant values of the remaining parameters, which are: the damping coefficients $c_1 = 0{\cdot}5$, $c_2 = 0{\cdot}05$, the normalized amplitude of the external harmonic excitation $f = 36$, the frequency of the external harmonic excitation $\omega = 2$, and $\beta = 1$. The initial conditions of the master system and the slave system are given as (1·0, 0·2) and (0·1,

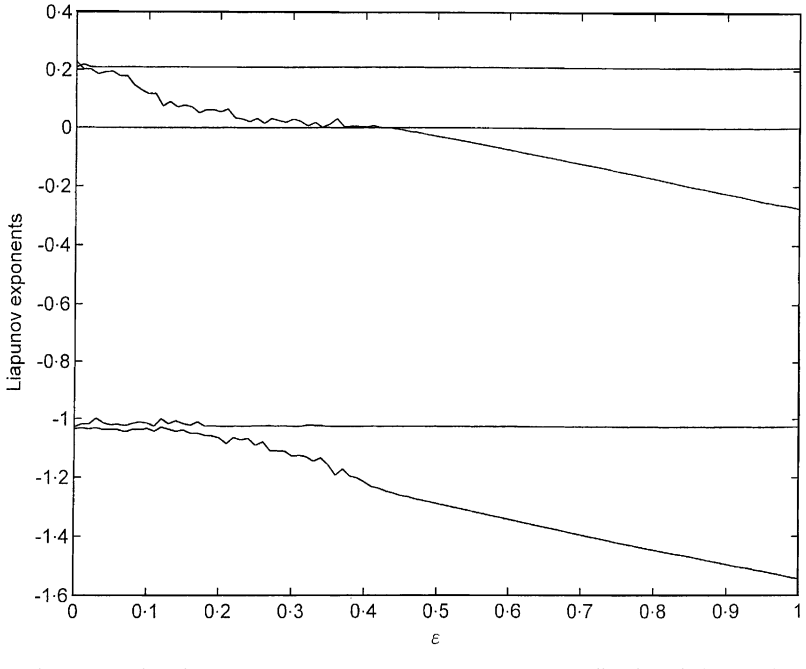

Figure 11. The Liapunov exponents versus ε as one-way coupling is $\varepsilon \sin(x_2 - y_2)$.

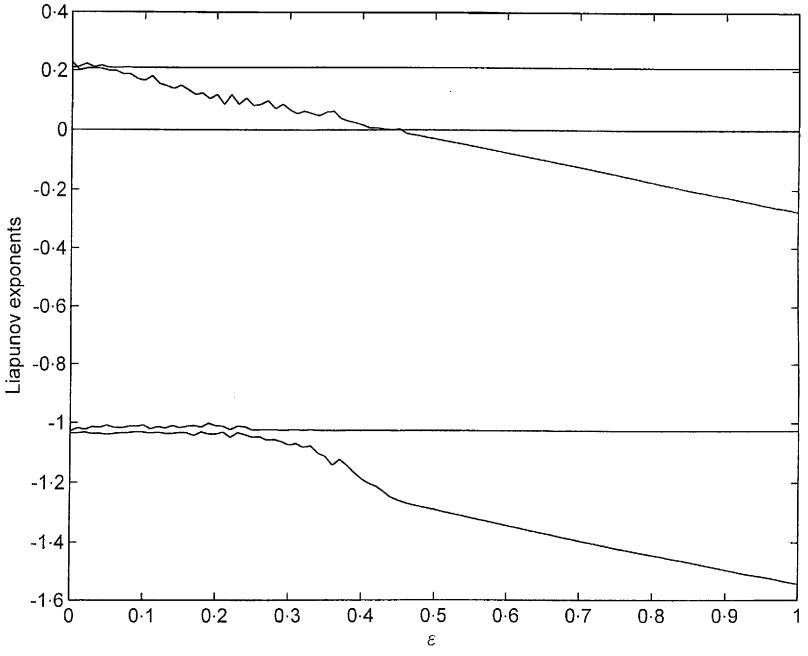

Figure 12. The Liapunov exponents versus ε as one-way coupling is $\varepsilon \sin(x_2 - y_2)$.

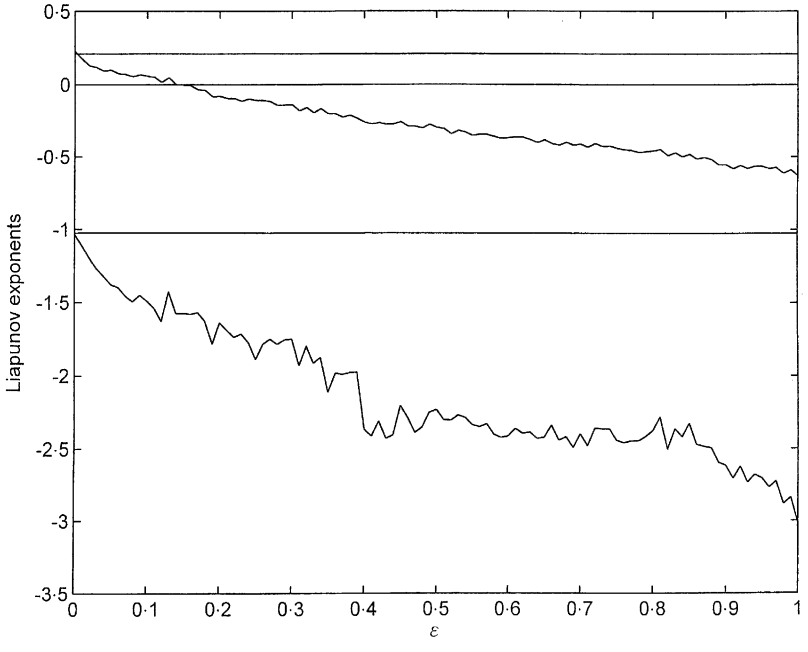

Figure 13. The Liapunov exponents versus ε as one-way coupling is $\varepsilon [\exp(x_2 - y_2) - 1]$.

0·02) respectively. In the present study, the whole system (master and slave) will be integrated numerically in order to obtain the Liapunov exponents. When the coupling parameter ε is not sufficient large, the type of the Liapunov exponents for the whole system is presented as $(+, +, -, -, 0)$. It implies that the hyper-chaotic attractor exists. As ε is

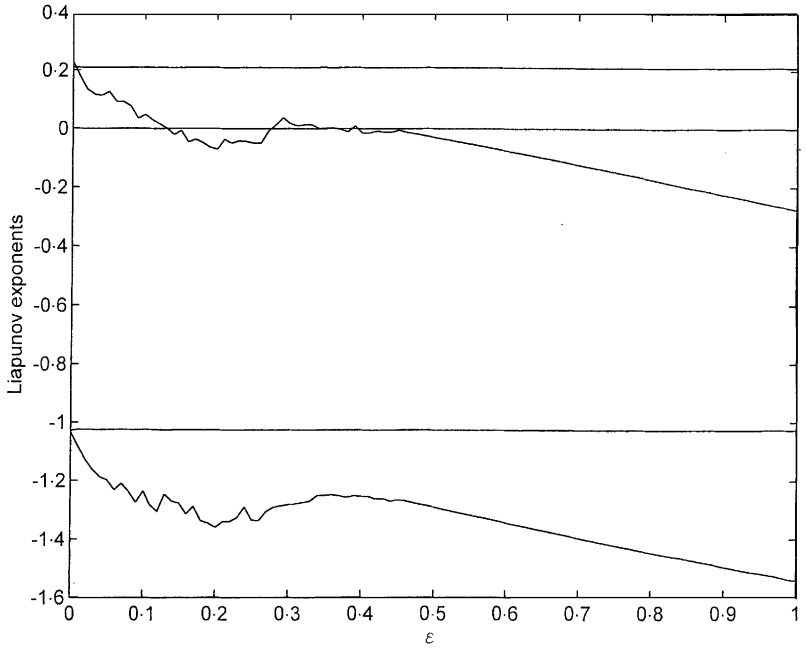

Figure 14. The Liapunov exponents versus ε as one-way coupling is $\varepsilon \sinh(x_2 - y_2)$.

increased further, an interesting phenomenon appears. The type of the Liapunov exponents is changed into $(+, -, -, -, 0)$. It implies that the two identical systems will be synchronized. The Liapunov exponents of the whole system for four different kinds of one-way coupling are shown in Figures 11–14, respectively.

For case (A), if $\varepsilon \geqslant 0{\cdot}44$, the phase portraits of the master and the slave are synchronized. Figure 15(a) depicts the trajectory of $(x_2 - y_2)$, for $\varepsilon = 0{\cdot}80$. Figure 15(b) shows the relation of x_2 and y_2 when synchronization occurs. Figure 15(c) and 15(d) display the trajectories of the master system and the slave system respectively. On the contrary, if $\varepsilon = 0{\cdot}2$, as shown in Figure 16, the two identical systems will not synchronize.

For case (B), if $\varepsilon \geqslant 0{\cdot}46$, the phase portraits of the master system and the slave system are synchronized. Figures 17 and 18 show the synchronized behavior for $\varepsilon = 0.8$ and unsynchronized behavior for $\varepsilon = 0{\cdot}2$, respectively.

For case (C), if $\varepsilon \geqslant 0{\cdot}14$, the phase portraits of the master system and the slave system are synchronized. Figures 19 and 20 show the synchronized behavior for $\varepsilon = 0{\cdot}80$ and unsynchronized behavior for $\varepsilon = 0{\cdot}1$ respectively.

For case (D), Figure 14 shows an interesting phenomenon. The sub-Liapunov exponent transverses zero many times in certain interval of ε. Therefore, the detailed discussion is needed. It is found that the major sub-Liapunov exponent is negative at $\varepsilon \in [0{\cdot}14\text{–}0{\cdot}27, 0{\cdot}37, 0{\cdot}38]$ and $\varepsilon \geqslant 0{\cdot}40$. The master system and slave system are calculated by numerical integration for $\varepsilon \in [0{\cdot}14\text{–}0{\cdot}27, 037, 0{\cdot}38]$. The incremental value of ε is 0·01. A fascinating behavior of the slave system is observed during the integration process. The attractor of the slave system is changed into another configuration. The attractor of the slave system is also changed depending on the value of ε while $\varepsilon \in [0{\cdot}14\text{–}0{\cdot}27]$. Further, as $\varepsilon = 0{\cdot}37$ and 0·38, the strange attractors of the slave system are still different from the master's strange attractor. It is clear that synchronization will not be present. The Poincaré maps of the slave system are also shown in Figure 21(a)–21(d) for $\varepsilon = 0{\cdot}14$, $\varepsilon = 0{\cdot}18$, 0·27 and 0·38 respectively. Those

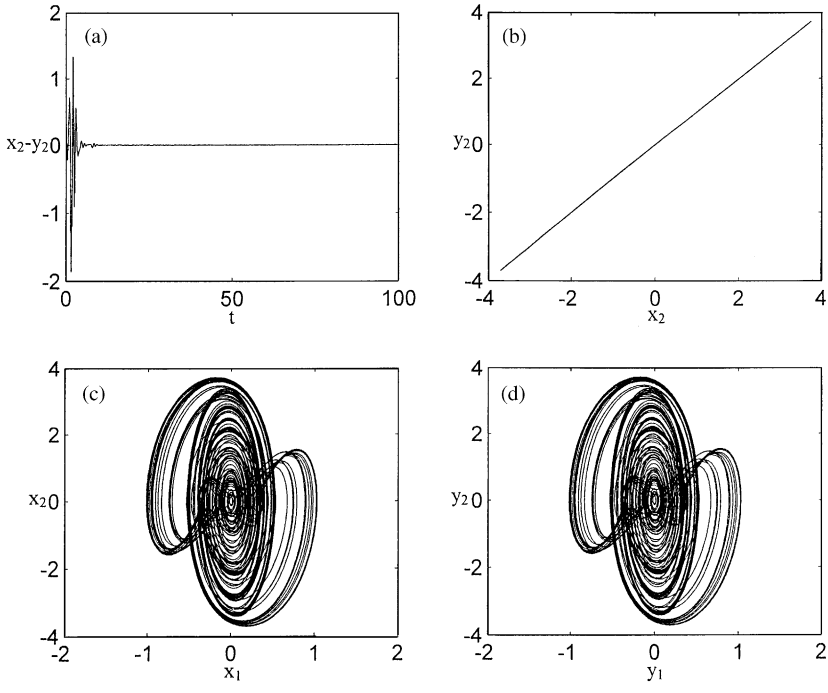

Figure 15. (a) The trajectory of $(x_2 - y_2)$; (b) The relation of x_2 and y_2; (c) The trajectories of the master system; (d) The trajectories of the slave system (synchronized motion for $\varepsilon = 0{\cdot}8$ in case (A)).

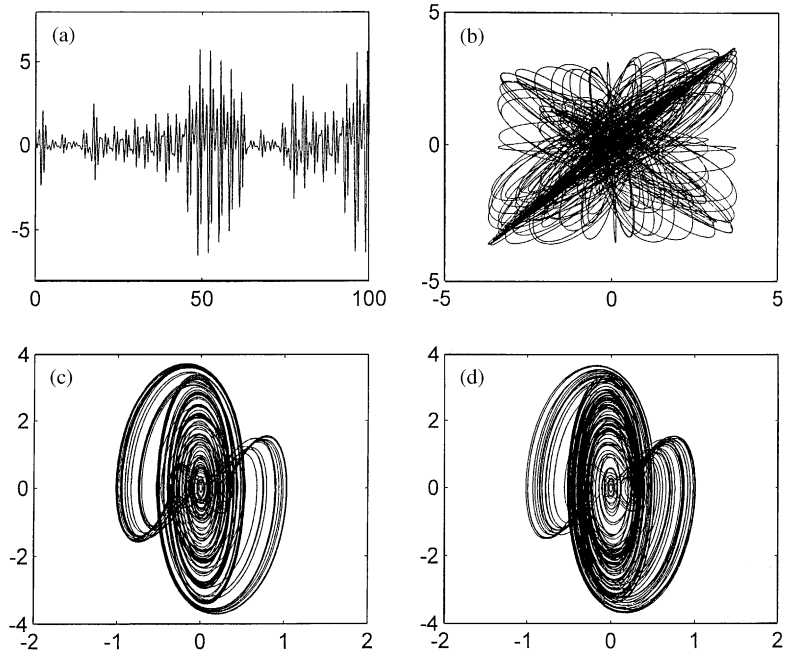

Figure 16. (a) The trajectory of $(x_2 - y_2)$; (b) The relation of x_2 and y_2; (c) The trajectories of the master system; (d) The trajectories of the slave system (unsynchronized motion for $\varepsilon = 0{\cdot}2$ in case (A)).

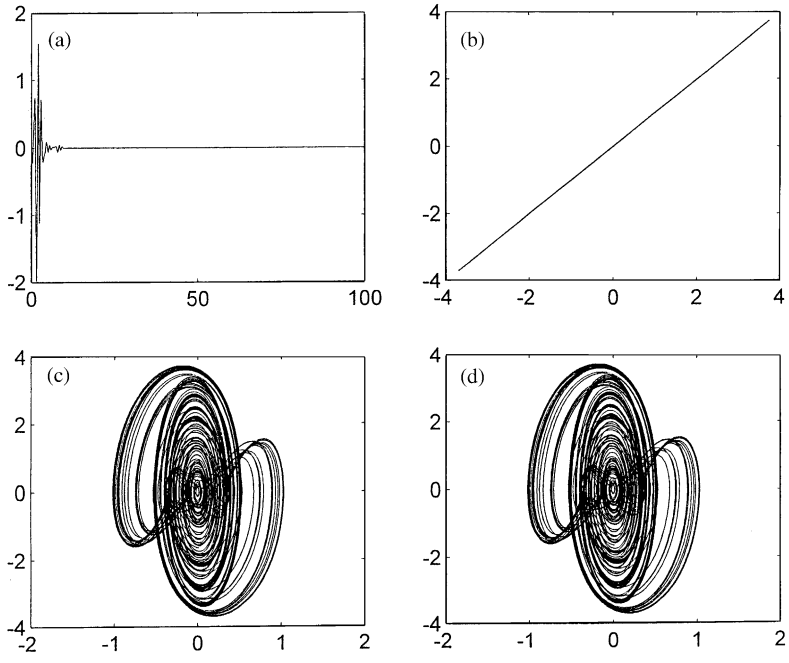

Figure 17. (a) The trajectory of $(x_2 - y_2)$; (b) The relation of x_2 and y_2; (c) The trajectories of the master system; (d) The trajectories of the slave system (synchronized motion for $\varepsilon = 0{\cdot}8$ in case (B)).

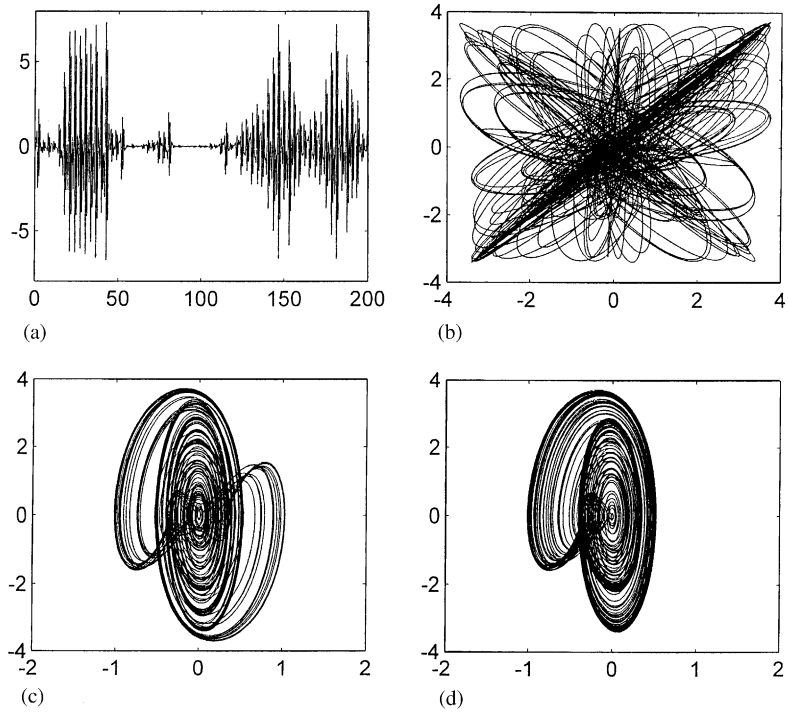

Figure 18. (a) The trajectory of $(x_2 - y_2)$; (b) The relation of x_2 and y_2; (c) The trajectories of the master system; (d) The trajectories of the slave system (unsynchronized motion for $\varepsilon = 0{\cdot}2$ in case (B)).

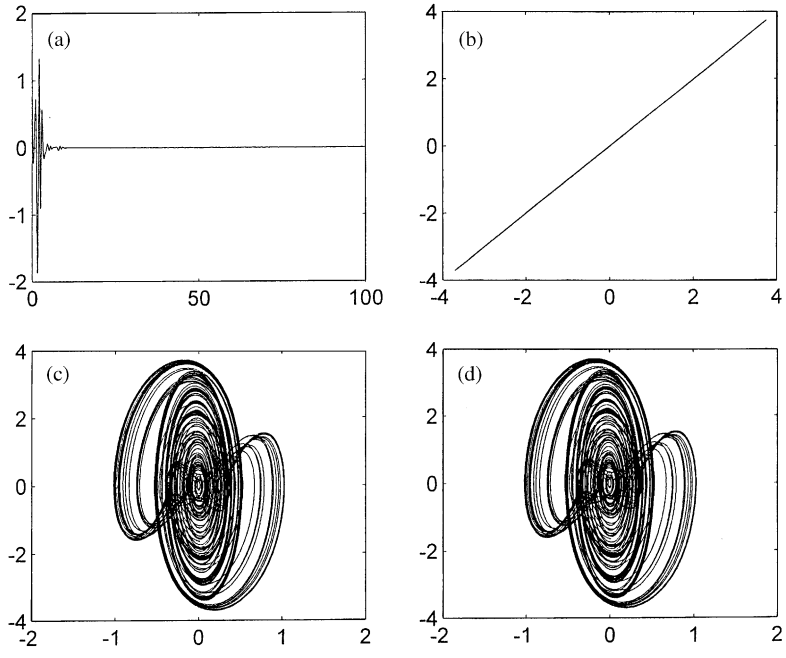

Figure 19. (a) The trajectory of $(x_2 - y_2)$; (b) The relation of x_2 and y_2; (c) The trajectories of the master system; (d) The trajectories of the slave system (synchronized motion for $\varepsilon = 0{\cdot}8$ in case (C)).

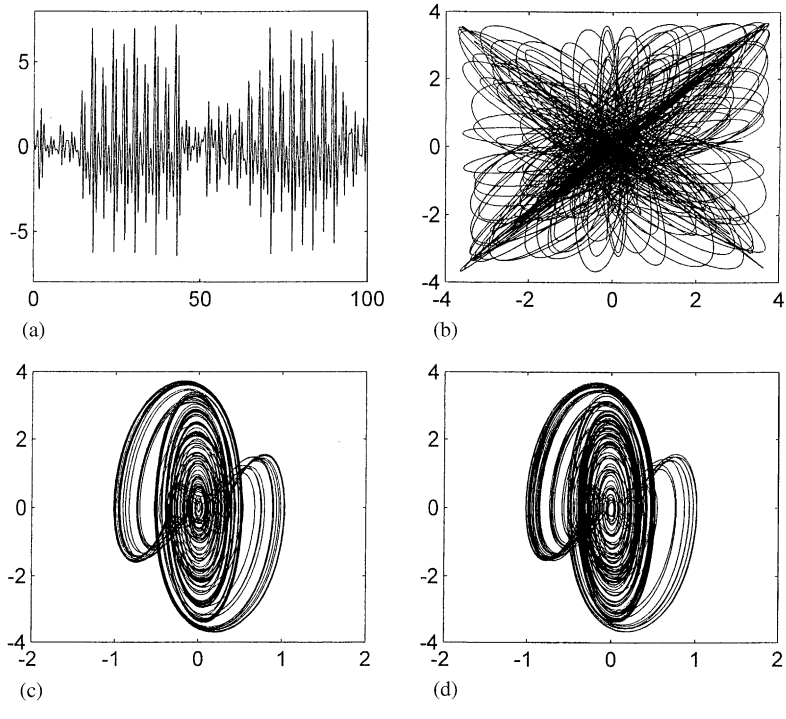

Figure 20. (a) The trajectory of $(x_2 - y_2)$; (b) The relation of x_2 and y_2; (c) The trajectories of the master system; (d) The trajectories of the slave system (unsynchronized motion for $\varepsilon = 0{\cdot}1$ in case (C)).

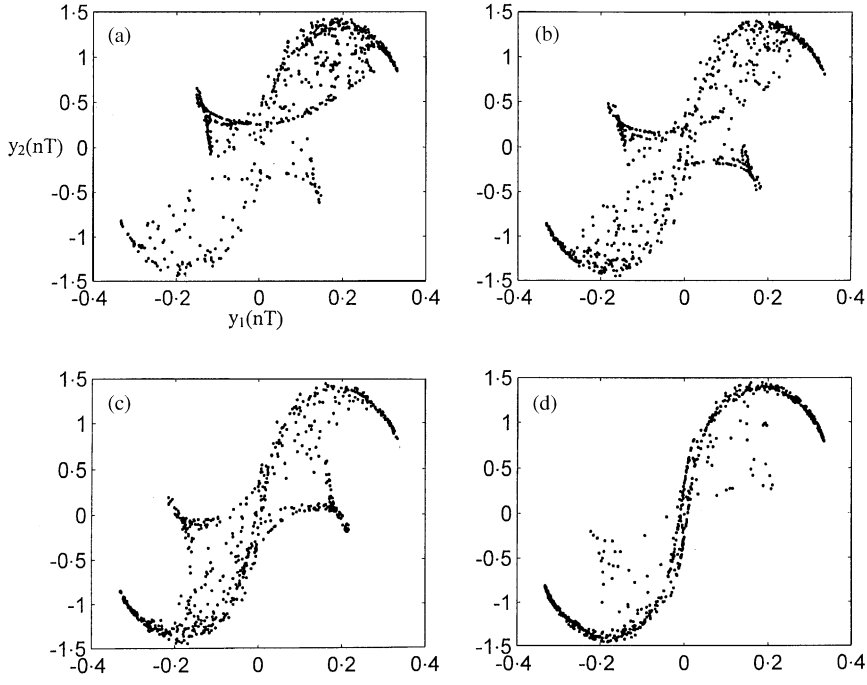

Figure 21. The Poincaré maps of the slave system for (a) $\varepsilon = 0{\cdot}14$, (b) $\varepsilon = 0{\cdot}18$, (c) $\varepsilon = 0{\cdot}27$ and (d) $\varepsilon = 0{\cdot}38$.

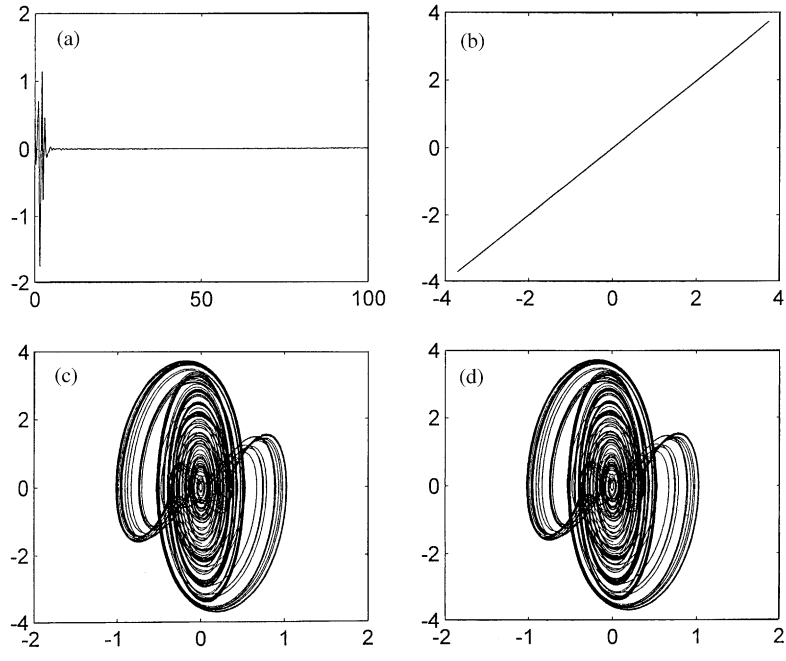

Figure 22. (a) The trajectory of $(x_2 - y_2)$; (b) The relation of x_2 and y_2; (c) The trajectories of the master system; (d) The trajectories of the slave system (synchronized motion for $\varepsilon = 0{\cdot}8$ in case (D)).

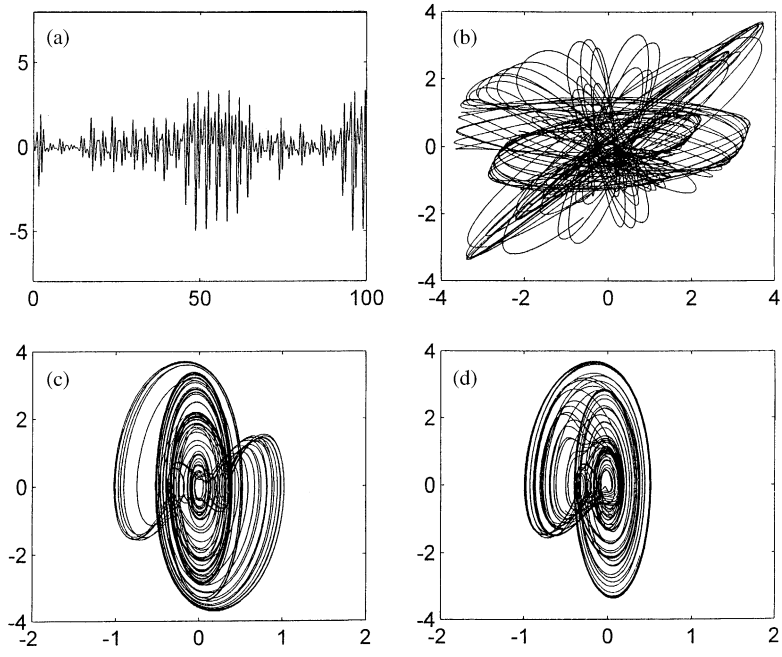

Figure 23. (a) The trajectory of $(x_2 - y_2)$; (b) The relation of x_2 and y_2; (c) The trajectories of the master system; (d) The trajectories of the slave system (unsynchronized motion for $\varepsilon = 0{\cdot}2$ in case (D)).

figures can be compared with the strange attractor presented in Figure 5(c). Finally, if $\varepsilon \geqslant 0{\cdot}4$, the phase portraits of the master and the slave are synchronized. Figures 22 and 23 show the synchronized behavior for $\varepsilon = 0{\cdot}80$ and the unsynchronized behavior for $\varepsilon = 0{\cdot}20$ respectively. Hence, when applying the one-way coupling we know that the behavior of the slave system is dependent on the behavior of the master system. However, the master system is not influenced by the behavior of the slave system.

From the paragraph above, four kinds of one-way coupling have been successfully applied to obtain chaos synchronization in the two identical systems. The next step is to evaluate the time required for a chaotic trajectory of the slave system to synchronize with a chaotic trajectory of the master system with a one-way coupling alone. For this purpose, an error function is defined by

$$E(t) = |x_1 - y_1| + |x_2 - y_2| + |\dot{x}_1 - \dot{y}_1| + |\dot{x}_2 - \dot{y}_2|. \tag{30}$$

When the value of $E(t)$ is less than 10^{-6}, the synchronization of these two identical systems are achieved. The time t which corresponds to $E(t) < 10^{-6}$ is called the "synchronization time". According to the above rigorous definition, if $\varepsilon = 0{\cdot}80$, the synchronization times for cases (A), (B), (C), and (D) are 53·02 s, 53·29 s, 52·87 s and 52·54 s, respectively.

8. CONCLUSIONS

The non-linear motion of a symmetric gyro with linear-plus-cubic damping mounted on a vibrating base has been investigated. It has shown that the system exhibits both regular and chaotic motions. Period-doubling route to chaos in this system is also observed. The

Liapunov direct method has also seen employed in a rigorous treatment of sufficient conditions for system stability. The bifurcation of the parameter-dependent system has been studied numerically. The time evolutions of the non-linear dynamical system response were described using the phase portraits via the Poincaré map technique. Further, the occurrence and nature of chaotic attractors have been verified by evaluating the Liapunov exponents and the Liapunov dimensions. Besides, several control methods, the delayed feedback control, the addition of the constant motor torque, the addition of the periodic force, and adaptive control algorithm (ACA), are successful by using to control chaos. The synchronization of chaos in the two identical chaotic motions of symmetric gyros is also studied. According to the results, two identical chaotic systems can be synchronized by applying four different kinds of one-way coupling. Finally, the synchronization time is also examined. This obviously is of significance for the design of future gyroscopes.

ACKNOWLEDGMENTS

This research was supported by the National Science Council, Republic of China, under Grant Number NSC 89-2212-E-164-003.

REFERENCES

1. R.-B. LEIPNIK and T.-A. NEWTON 1981 *Physics Letters* **86A**, 63–67. Double strange attractors in rigid body motion with feedback control.
2. Z.-M. GE, H.-K. CHEN and H.-H. CHEN 1996 *Journal of Sound and Vibration* **198**, 131–147. The regular and chaotic motions of a symmetric heavy gyroscope with harmonic excitation.
3. Z.-M. GE and H.-K. CHEN 1996 *Japanese Journal of Applied Physics* **35**, 1954–1965. Stability and chaotic motions of a symmetric heavy gyroscope.
4. X. TONG and N. MRAD 2001 *Transactions of American Society of Mechanical Engineers, Journal of Applied Mechanics* **68**, 681–684. Chaotic motion of a symmetric gyro subjected to a harmonic base excitation.
5. H. POINCARÉ 1899 *Les Methodes Nouvelles De La Mecanique*. Paris: Gauthier-Villiars.
6. E.-N. LORENZ 1963 *Journal of Atmospheric Science* **20**, 130–141. Deterministic non-periodic flow.
7. Y. BRAIMAN and I. GOLDHIRSH 1991 *Physical Review Letters* **66**, 2545–2548. Taming chaotic dynamics with weak periodic perturbations.
8. E. OTT, C. GREBOGI and J.-A. YORKE 1990 *Physical Review Letters* **64**, 1196–1199. Controlling chaos.
9. B.-A. HUBERMAN and E. LUMER 1990 *IEEE Transactions on Circuits and Systems* **37**, 547–550. Dynamics of adaptive system.
10. L.-M. PECORA and T. L. CARROLL 1990 *Physical Review Letters* **64**, 821–824. Synchronization in chaotic systems.
11. M. LAKSHMANAN and K. MURALI 1996 *Chaos in Nonlinear Oscillators: Controlling and Synchronization*. Singapore: World Scientific.
12. F.-R. GANTMACHER 1960 *Lectures on Analytic Mechanics* (Gosudarstvennoe Izdat'elstvo FizikoMat'emat'iskoi Literaturi, Moscow, 1960) (in Russian).
13. M. VIDYASAGAR 1993 *Nonlinear Systems Analysis*. London: Prentice-Hall.
14. L. CVETICANIN 1995 *Transactions of American Society of Mechanical Engineers, Journal of Applied Mechanics* **62**, 227–229. A note on the stability and instability of system with time variable parameters.
15. A. WOLF, J.-B. SWIFT, H.-L. SWINNEY and J. A. VASTANO 1985 *Physica* **16 D**, 285–317. Determining Liapunov exponents from a time series.
16. P. FREDERICKSON, J.-L. KAPLAN, E.-D. YORKE and J.-A. YORKE 1983 *Journal of Differential Equations* **49**, 185–207. The Liapunov dimension of strange attractors.